OPEN CHANNEL NOISE

III. High-Resolution Recordings Show Rapid Current Fluctuations in Gramicidin A and Four Chemical Analogues

F. J. SIGWORTH,* D. W. URRY,‡ AND K. U. PRASAD‡

**Department of Physiology, Yale School of Medicine, New Haven, Connecticut 06510 and Abteilung Membranbiophysik, Max-Planck-Institut für biophysikalische Chemie, Göttingen, Federal Republic of Germany; ‡Laboratory of Molecular Biophysics, University of Alabama at Birmingham School of Medicine, Birmingham, Alabama* 35294

ABSTRACT Using a technique for high-resolution recording of currents from lipid bilayers, we have measured the current fluctuations in open channels formed by gramicidin A (GA) and the four analogues L-Ala^7-GA, L-Leu^5-GA, con D-Leu^{5a}-L-Ala^{5b}-GA and, des-L-Val^7-D-Val^8-GA. Over the frequency range 40 Hz–20 kHz the fluctuations in each type of channel showed flat (frequency independent) spectral densities which ranged from 1.1 to 2.4 times the value expected from shot noise. Larger values were obtained at 200 mV membrane potential than at 100 mV, and with 200 mM CsCl than with 1 M CsCl as the bath solution. A likely explanation for the excess noise would be the existence of brief interruptions in the channel current lasting <3 μs.

INTRODUCTION

The current through an open ionic channel is not expected to be steady, but will show fluctuations due to "shot noise" (Schottky, 1918), reflecting the fact that the current involves the movement of discrete charges across the membrane. Previous studies on the single-channel current fluctuations ("open-channel noise") in acetylcholine receptor channels (Sigworth 1985, 1986) have shown excess fluctuations above the level expected for shot noise, and this excess was thought to arise from fluctuations in the conformation of the channel protein. Since the three-dimensional structure of the acetylcholine receptor channel is not yet known, it will be some time before we can relate the observed fluctuations to parts of the protein structure. For this reason we have turned to the simpler channel protein gramicidin A (GA), for which much more is known about the channel structure as well as the mechanism of transport of ions through the channel (Urry, 1971; Urry et al., 1971; Hladky and Haydon, 1972; Andersen, 1984; Hladky and Haydon, 1984; Urry 1985*a*, *b*; Urry et al., 1988). Further, it has been possible to synthesize a number of chemical analogues of GA which show altered channel characteristics and which undoubtedly differ in their intramolecular motions. We report here the study of open-channel noise in GA (Fig. 1) and in four analogues: L-Ala^{7}GA (Prasad et al., 1986); L-Leu^5-GA (Urry et al., 1984*a*); con D-Leu^{5a}-L-Ala^{5b}-GA (Prasad, K., and D. Urry, manuscript in preparation); and des-L-Val^7-Val^8-GA (Urry et al., 1984*b*). We find that each of these channel types shows excess noise which probably arises from conformational fluctuations, but no spectral features are visible in the frequency range below 20 kHz, implying that the fluctuations are rapid in each case.

Please address correspondence to F. J. Sigworth, Department of Physiology, Yale School of Medicine, 333 Cedar Street, New Haven, CT 06510

METHODS

Synthesis of Gramicidin A and Selected Analogues

(1-^{13}C)-Val^1-Gramicidin A used in the current studies was prepared from the natural Gramicidin mixture obtained from ICN Pharmaceuticals, Inc., Irvine, CA. After deblocking the formyl group, the NH_2-terminal Val was removed by the standard procedures of Edman degradation and the resulting des-formyl-des-valyl^1-GA was coupled with formyl-(1-^{13}C)-L-Val-*p*-nitrophenyl ester to obtain (1-^{13}C)-Val^1-GA which was purified by passing through a mixed-bed resin column and then through an AG50W-X2 (Bio-Rad Laboratories, Richmond, CA) ion-exchange column. Further purification was achieved by preparative thin-layer chromatography (TLC) and LH-20 column chromatography. At this stage the peptide was demonstrated to be at least 90% pure by means of carbon-13 nuclear magnetic resonance (CMR) spectra. Final purification of the sample was carried out by high performance liquid chromatography (HPLC). The sample was passed through an analytical reverse phase C-18 column several times. Each time, the central portion of the peak was collected and repeatedly re-injected into the column. The same final purification by HPLC was carried out for all the samples used in this study. L-Leu^5-GA (Urry et al., 1984*a*), des-L-Val^7-D-Val^8-GA (Urry et al., 1984*b*), and L - Ala^7-GA (Prasad et al., 1986) were synthesized and purified as reported earlier. Con-D-Leu^{5a}-L-Ala^{5b}-GA was synthesized by the solid-phase methodology as described earlier (Prasad et al., 1982). The peptide was purified by preparative thin-layer chromatography followed by LH-20 column chromatography to more than 90% purity as was evident by CMR spectroscopy. The analogue was then subjected to HPLC purification as mentioned above for use in the present studies. The

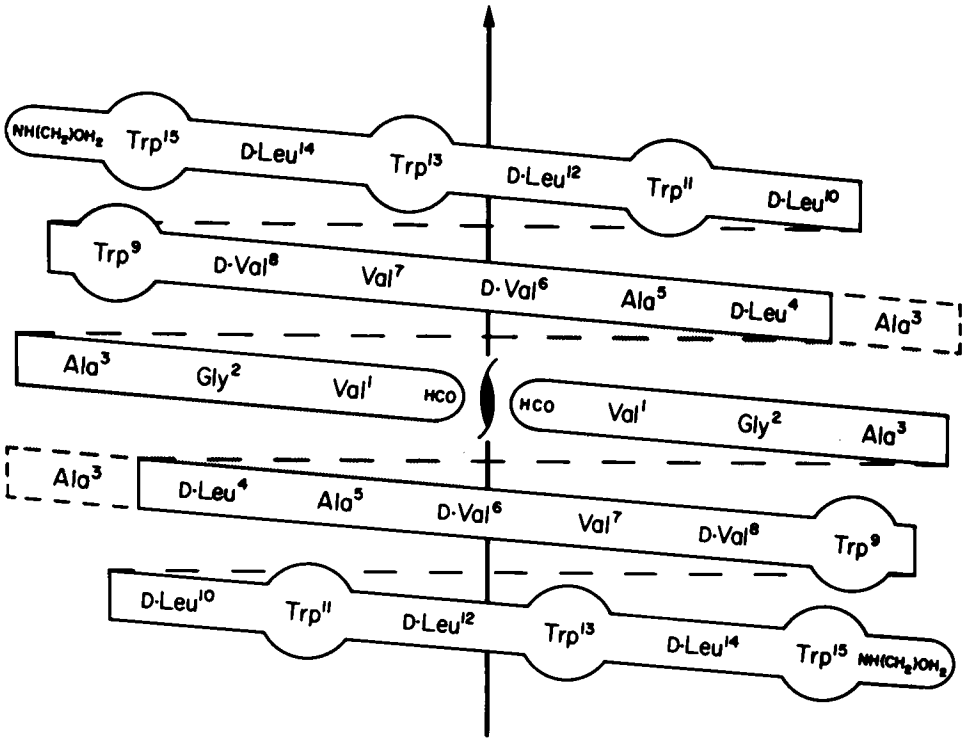

FIGURE 1 Schematic structure of the gramicidin A dimer. The NH_2-termini of the two 15-residue polypeptide chains are blocked by formyl groups and are found at the junction between the two monomers (center of figure). The area of contact between two monomers shown is shaded. The COOH-termini (*upper left* and *lower right*) are blocked by ethanolamine groups. In the L-Ala[7] analogue, Val[7] was replaced by the smaller alanine, with the intention of providing less steric hindrance for the large side chain of Trp[13]. Conversely, the L-Leu[5] analogue replaces Ala[5] with leucine to provide more hindrance for Trp[11]. The con D-Leu[5a]-L-Ala[5b] analogue introduces an extra Leu-Ala pair after Ala[5], while the des L-Val[7]-D-Val[8] analogue removes those two residues.

verification of synthesis of the con D-Leu[5a]-L-Ala[5b]-GA synthesis has been presented elsewhere.

Formation of Micro-Bilayers. Black lipid membranes were formed and transferred to the tips of glass pipettes by a technique similar to the one of Andersen (1983) and developed for us by E. Neher. A 1-mm Teflon tube is first partly filled with bath solution by suction, and then a lipid film is formed at its mouth by passing it through the air-water interface where a small amount of lipid-hydrocarbon solution has been spread. With the tube held in the bath a bubble of lipid is then formed by displacing some solution from the tube (Fig. 2). The lipid-solvent film in the bubble spontaneously thins to form a hemispherical bilayer.

The recording pipette is similar to a standard patch-clamp pipette, and can be fabricated in the usual way, using a microelectrode puller (Hamill et al., 1981). However, we obtained higher seal resistances and more stable membranes when the pipettes were pulled on a microforge (see Neher et al., 1978) using a freshly glass-coated filament, probably because less metal is deposited on the glass in that technique. Pipettes were coated with Sylgard, heat polished, and then their tips were silanized by dipping them briefly into a 10% solution of trioctylsilane or dimethyldichlorosilane. Most of the recordings were made using thin-walled borosilicate glass capillaries (Kimax). Slightly lower noise levels but less stable membranes were obtained using aluminosilicate glass (Hilgenberg).

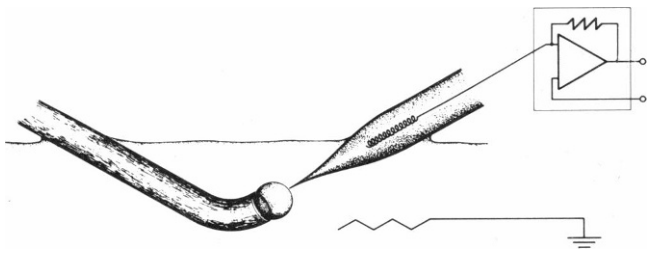

FIGURE 2 Recording system. Lipid-decane suspension is spread on the opening of a solution-filled Teflon tube and a "bubble" is formed which serves as the source of lipid for the tip of a glass pipette. The pipette is coated with Sylgard[R] and is attached to a standard patch-clamp amplifier. The bath and pipette electrodes are Ag-AgCl wires.

After a few attempts in which the bubble usually broke when touched by the pipette, the pipette could be repeatedly inserted into the bubble membrane without disturbing it. Then, a pulse of pressure applied to the pipette cleared out any lipid in the tip and allowed the "whole bubble" current to be monitored. In the absence of added gramicidin we observed bubble resistances around 10^9 Ω, which decreased to ~10^7Ω when gramicidin was added from an ethanol stock solution to give a suitable level of single-channel activity in the patch membrane. Typically, an aliquot ~10 μl of 10^{-8} to 10^{-9} M gramicidin in ethanol was added to the 2 ml of bath solution.

To obtain a low background noise level we used smaller pipettes than Andersen (1983), typically 2–5 μm tip diameter and having resistances ~200 kΩ in 1 M CsCl. Pipettes with ~2 μm or smaller tips tended to clog easily with lipid, while pipettes larger than 5 μm gave substantially higher noise levels due to the larger membrane capacitance. Clogged pipettes could often be cleared by applying slight suction to them; what resulted in many cases was an abrupt increase in capacitance and the appearance of channel activity. We believe that these changes reflect the pulling of the lipid plug up into the pipette and its subsequent thinning into a bilayer. Small changes in the applied pressure can then change the membrane area (measured as capacitance) as the membrane and its solvent torus ride up into the wider shank of the pipette or shrink as they move toward the tip. In a typical recording situation the membrane capacitance was typically 0.1 pF and the background noise was 200 fA rms (in the frequency band 0.3 – 3 kHz), slightly higher than the ~160 fA noise level that can be obtained with similar pipettes and the EPC-7 amplifier in patch-clamp recordings from cell membranes.

Pipettes could be used and reused for several days after fabrication. Between experiments they were washed by aspirating water, methanol, and hexane. (The chloroform-methanol wash that was normally used for other parts of the apparatus was avoided because of deterioration of the Sylgard[R] coating in this solvent).

In the experiments described here the lipid was diphytanoyl phosphatidylcholine (Avanti Polar Lipids, Inc., Birmingham, AL), 20 mg/ml in

decane. The bath solutions were unbuffered 1 M or 0.2 M CsCl solutions (pH near 6.2). All experiments were performed at room temperature (~25°C).

Current Recording and Analysis. The pipette current was monitored with an EPC-7 patch clamp (List Medical, Darmstadt, FRG), whose internal Bessel filter was set to 10 kHz (−3 db frequency). The current monitor signal was recorded using one of the two data channels of a modified PCM-701 digital audio processor (Sony Corp. of America, Long Island City, NY) and a VHS video recorder. The modifications to the PCM-701 were similar in principle to those described by Bezanilla (1985). The internal record and playback anti-aliasing filters were replaced by 17 kHz, 4-pole filters (E. Butterworth) for improved transient response and precision current references were provided for the internal A-D and D-A converters.

For data analysis the digital data stream obtained from playback of the tape was converted to 16-bit parallel words (Bezanilla, 1985), read into computer memory through a DMA interface, and written directly to a 16-megabyte disk file. This file would hold 180 seconds of continuous data, sampled at the rate of 44.1 kHz that is fixed by the PCM-701.

The evaluation of open-channel noise power spectra proceeded by the same general strategy as described previously (Sigworth, 1985): the raw data were scanned to detect brief channel closures, which were then masked to avoid contaminating the spectra. Average spectra were then accumulated from periods of baseline and periods when one, two, or more channels were open. Because of the large amount of data resulting from each recording an automatic program performed the time-consuming masking and FFT operations, and reduced the stored information to a set of files totaling 1 megabyte in size. This program operated on blocks of 4,096 data samples (~100 ms of recording). It first filtered and decimated these to blocks of 128 "compressed" data points to provide an overview of the time course of the mean current. Then brief channel transitions were masked before spectra were computed from each block of points. The masking threshold was set to be the smaller of either ±5 times the standard deviation σ_n of the masked data (at the 10-kHz bandwidth the value of σ_n was typically ~0.7 pA), or a fixed upper limit that was set manually. In the masking operation, the data samples comprising the neighborhood of each masked event were set to the average value of all unmasked samples in the block by means of an iterative algorithm (Sigworth, 1985). This technique reliably eliminated channel turn-on and turn-off events as well as brief closures in the cases of large (>8 pA) channel currents at the full recording bandwidth. To mask transitions in channel events whose amplitude was smaller than $5\sigma_n$, each block of 4,096 events was first processed by a Gaussian filter (Colquhoun and Sigworth, 1983) to reduce the background noise level. From these filtered data the points to be masked were determined, and then the corresponding points were masked on the full-bandwidth data before spectral analysis was performed on the latter. The effective bandwidth of the Gaussian filter was set at 2 or 4 kHz.

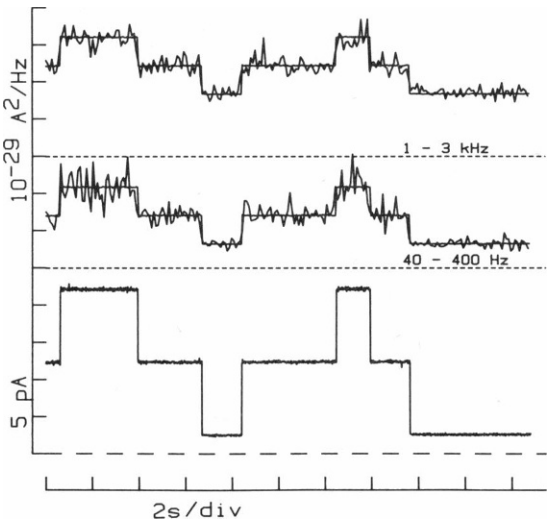

FIGURE 3 Time course of the mean current and variance. The lowest trace is the current from Ala[7] channels in 200 mM Cs at 200 mV; the vertical scale is 5 pA per division. The two noisy upper traces are average spectral density estimates obtained from each 100 ms of the record by averaging the spectral values in the frequency ranges indicated; the vertical scale is $10^{-29}A^2/Hz$ per division. Superimposed on the two spectral density traces are identically scaled copies of the current trace, showing the close correspondence of the time courses of mean and variance.

From each 4,096-point block two complex FFT operations were used to compute four power spectra, which in turn were averaged and a correction was made for the attenuation of high frequencies by the filters and recording system. The higher-frequency spectral values were then pooled to result in 64 floating-point spectral estimates. Also from each block of masked data a 128-point amplitude histogram was computed. For each 180-s recording this program required 6 h of computation time on a PDP-11/23 computer or 2 h on a PDP-11/73 (Digital Equipment Corp., Marlboro, MA).

After this computational effort it remained only to sort and accumulate the spectra according to the number and conductance level of channels open during the record. This was done with the help of a display of the time course of the mean current and the average spectral density in three frequency bands. The spectral density traces showed up artifacts due to masking errors or drifts in the background noise level. Fig. 3 shows such a display in which orderly increases in the spectral densities are seen to accompany increases in the number of open channels.

RESULTS

Single-Channel Currents in Gramicidin Analogues

Fig. 4 shows representative current traces obtained in 1 M CsCl solutions and 200 mV applied potential with gramicidin A (GA) and the four analogues that were used in this study. The L-Ala[7] and L-Leu[5] analogues have already been shown to have channel lifetimes and primary conductance levels similar to those of GA (Prasad et al., 1986; Urry et al., 1984*a*; Venkatachalam et al., 1984). The con-D-Leu-L-Ala analogue has longer channel lifetimes, as would be expected from the effect of relative membrane thickness on lifetime (see for example Hladky and Haydon, 1984). Similarly the physically shorter des-L-Val[7]-D-Val[8] analogue has a greatly shortened open time and also reduced conductance (in 1M KCl as well: see Urry et al, 1984b). In the decane-PC membranes that we used the mean channel lifetimes for GA, Ala[7]-GA, and Leu[5]-GA were all ~5 seconds, and they showed primary conductance levels of 45–46 pS in 1 M CsCl and 100 mV. The lifetime of the con-D-Leu-L-Ala derivative was so long, at least an order of magnitude longer, that recording single channel events was difficult. In the single event shown the conductance was 20 pS. The des-Val[7]-Val[8] analog had a mean open time of 110 ms and a conductance of 40 pS.

Brief Gaps

As was shown by Ring (1986), GA channels in glycerol-monooleate membranes show brief (~1 ms duration) inter-

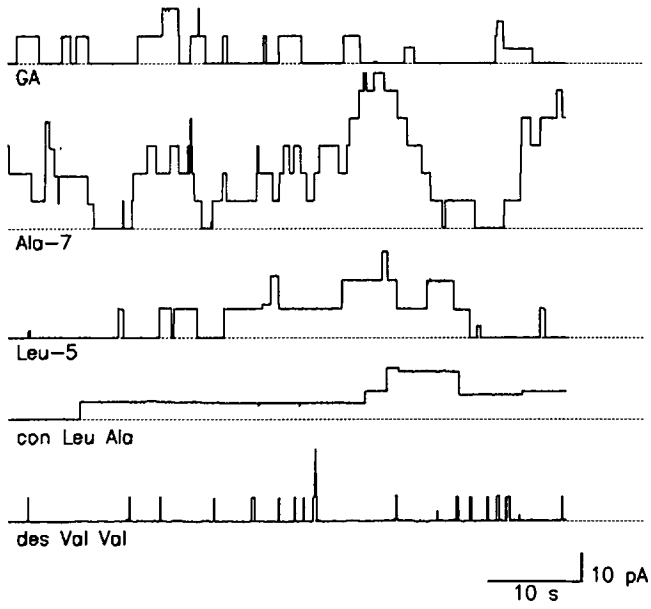

FIGURE 4 Representative current traces from the various GA analogues in 1 M CsCl and 200 mV. GA and the Ala[7] and Leu[5] analogues have essentially the same main current level of 8.9 pA, but Ala[7] shows fewer lower-conductance "mini-channel" events, while Leu-5 shows relatively more of them. The con Leu-Ala analogue has currents of 5.7 pA but much longer lifetimes, while the des Val[7]-Val[8] analogue has currents of 7.9 pA and decreased lifetimes.

ruptions in the channel current. We observed similar "gaps" in our records, but they tended to be shorter than those reported by Ring and their frequency of occurrence was quite variable. Fig. 5 shows representative gaps from a GA recording at 200 mV, and Fig. 6 shows the statistics of gaps from this recording and a recording from Ala[7] channels, both of which had particularly high rates of occurrence. In Fig. 5 two classes of gaps can be distinguished: the shorter gaps had an apparent mean lifetime of 27 μs and occurred at a rate of $\sim 8\ s^{-1}$. The amplitude of most of these events could not be determined because they were not well resolved in our recordings (the minimum gap length for detection was 16 μs), but the longer ones of this class appeared to be complete interruptions of the channel current. Another class of gaps had a mean lifetime of ~300 μs and included a large number of partial closings of the channel, as illustrated in Fig. 5 *E*, and also were present in ~20% of the opening and closing transitions (Fig. 5 *F*). Other recordings had much lower rates of occurrence of the short gaps, on the order of $1\ s^{-1}$. The variability in rates may be due to an effect of the membrane thickness, where thicker membranes result in higher gap rates (Shenkel, S., and F. Sigworth, unpublished observations), and the membrane thickness could have varied depending on the solvent content of the membrane at the tip of the pipette.

Power Spectra: Controls

To obtain the power spectrum of fluctuations in channel currents, we accumulated average power spectra from

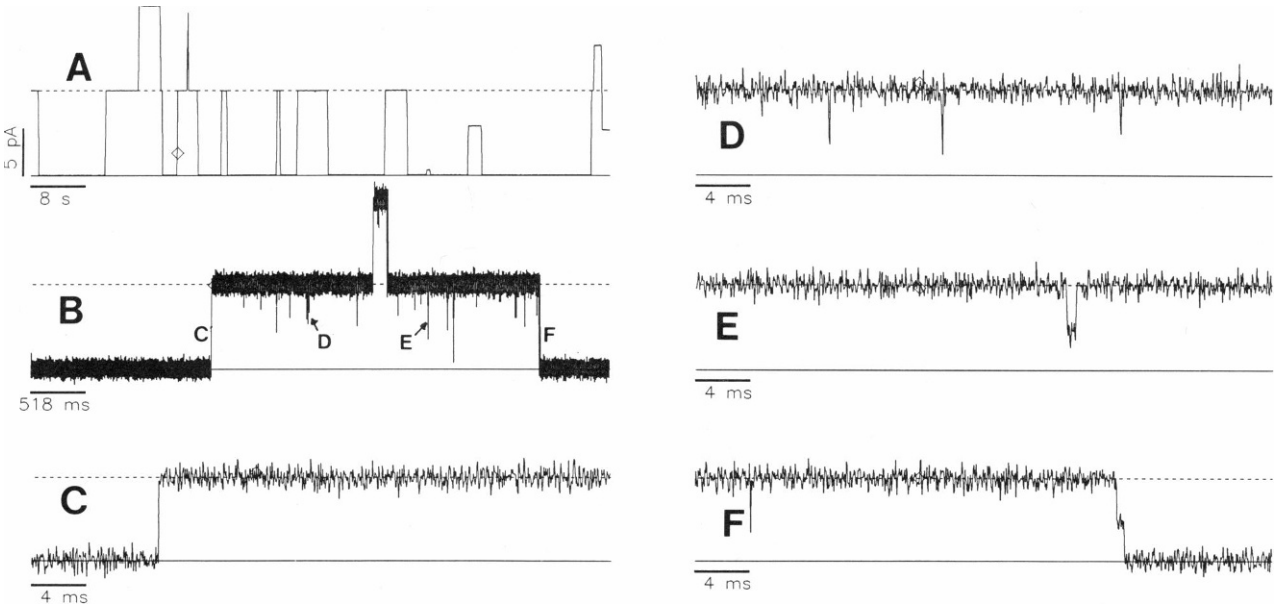

FIGURE 5 Brief conductance changes in GA currents in 1 M Cs and 200 mV. (*A*) Overview of currents at low time resolution. (*B*) Expansion by 16 of the event marked with a diamond in *A*, and displayed after Gaussian filtering at 5 kHz. The pulse in the middle of this 3-s event apparently results from the overlap of two channels of identical conductance. The rising and falling edges of the event as well as two regions containing "gaps" are shown in traces *C–F* as marked. (*C*) The rising edge of the current is instantaneous at the time resolution available. (*D*) Three short interruptions. Because they are so brief (~20 μs duration) it is not possible to determine whether they are reductions to a low conductance level or a complete interruption of the current, though many slightly longer gaps do reach the baseline. (*E*) A sojourn at approximately half the normal current for 0.36 ms. (*F*) A similar sojourn lasting 0.28 ms during the falling edge of the current pulse.

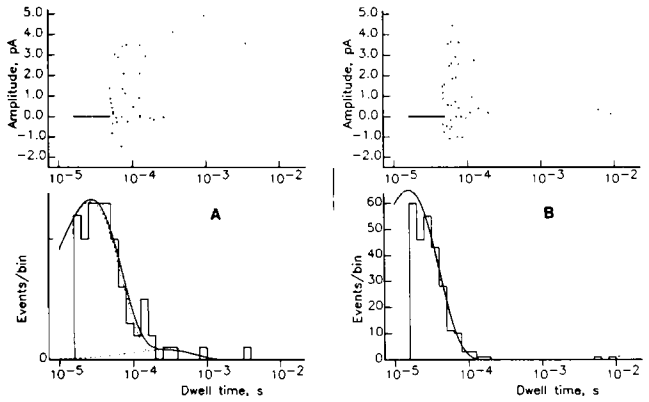

FIGURE 6 Statistics of gaps in, *A*, a recording of GA channels (same run as shown in Fig. 5) and *B*, a recording of Ala^7 channels in 200 mM Cs, 200 mV. In the upper plot the average current amplitude during the gap is plotted against the dwell time in the reduced current level (full channel current was 8.9 pA in *A*, 9.1 pA in *B*). Amplitude estimates were not made for gap durations <50 μs, so that these points are plotted with an amplitude of zero. The lower plots are histograms of all dwell times, binned according to the same logarithmic dwell-time axis (Sigworth and Sine, 1987). The fitted curves in *A* represent the sum of two exponential distributions, one with $\tau_1 = 27$ μs and with a total area $N_1 = 155$ events, and the other with tentative values of $\tau_2 = 270$ μs and $N_2 = 8$ events. The total open time analyzed was 18.9 s. In *B* the single exponential distribution had the parameters $\tau = 16$ μs and $N = 716$, for 33.6 s of total open time. The dwell times for short events were determined by the 50%-threshold crossing technique and were corrected according to the step response of the recording system (Colquhoun and Sigworth, 1983).

portions of recordings with no channels open and with one channel open, and subtracted them as shown in Fig. 7. As was pointed out in Sigworth (1985), this procedure yields the true spectrum of the channel provided that the open-channel current fluctuations are uncorrelated with any background fluctuations. A strong test for such correlations is shown in Fig. 7 *D*, where difference spectra obtained with one, two or three open channels are shown. For uncorrelated noise in the channels the spectral density is expected to increase proportionately with the number of channels, and this is seen to be the case. The spectral density of correlated noise, on the other hand, is expected to increase as the square of the number of channels. The fact that the spectral density obtained with three channels open is very close to three times the density from one channel therefore argues that any correlated noise component is negligible in size.

A second test of the noise measurement technique was to measure the equilibrium noise in a channel. At equilibrium the spectral density of the current noise in a channel is independent of the conductance mechanism and depends only on the channel conductance γ according to the Nyquist relation

$$S(f) = 4kT\gamma, \tag{1}$$

where k is Boltzmann's constant and T is the absolute temperature. We computed the difference spectrum of current noise in a GA channel in 1 M CsCl with 20 mV applied potential. This potential is close to equilibrium in the sense that ion transport noise, calculated as shot noise for monovalent ions, is expected to be at most about 7% larger than that given by Eq. 1. The resulting spectrum (Fig. 8) is seen to be flat and has the expected value, the same as the thermal noise in a 19 GΩ resistor.

Power Spectra from Gramicidin Analogues

Power spectra from the open-channel noise in GA channels and channels formed by analogues are shown in Figs. 9 and 10. Fig. 9 shows spectra obtained in 1 M CsCl and 200 mV applied potential. For GA and Leu^5 two spectra are shown, one from the main (most common) conductance state and one from a subconductance state. In each case the spectrum is essentially flat, and the spectral density is significantly higher than the classical shot noise density, which is indicated as a dashed line in each panel of the figure. The shot noise theory, which assumes a unidirectional flux of independently-moving ions across a potential difference, yields a spectral density that is independent of frequency (up to the frequency corresponding to the actual transit time of an ion through the channel) and which depends only on the single-channel current i and the magnitude of the charge q of the transported ions (Schottky, 1918; see Stevens, 1972; Läuger, 1974),

$$S_{\text{shot}}(f) = 2iq. \tag{2}$$

We use the spectral density given by Eq. 2 as a reference, and normalize each experimentally observed spectral density S_{av} by the S_{shot} value computed from the corresponding i to obtain the "noise ratio" r,

$$r = \frac{S_{\text{av}}}{S_{\text{shot}}}.$$

The experimental average spectral densities were computed from the spectral points in the range of 500 Hz to 5 kHz. The values of S_{av} are shown as a solid line in each panel of the figure. The most prominent difference among the analogues in Fig. 9 is seen to be between the GA and Ala^7 spectra, with r values near 1.3, and the Leu^5 spectrum, which had $r = 1.8$. A comparison of spectra obtained from different runs suggests that this difference is significant. The des-Val^7-Val^8 spectrum shows a low r value, but this value is quite uncertain.

When the salt concentration was reduced from 1 M to 200 mM the single-channel currents in GA and Leu^5 channels decreased to about half, but surprisingly the current in Ala^7 channels remained nearly the same—it actually increased slightly, from 8.9 to 9.3 pA, at 200 mV. This suggests that the conductance of Ala^7 channels reaches its maximum between these two concentrations, in contrast to GA where the maximum conductance in Cs occurs above 1 M. In 200 mM Cs the noise spectra (Fig. 10) from all of the analogues again appear to be flat, but all of the values of r are higher than in 1 M Cs. The most dramatic increase was for the GA and Ala^7 channels,

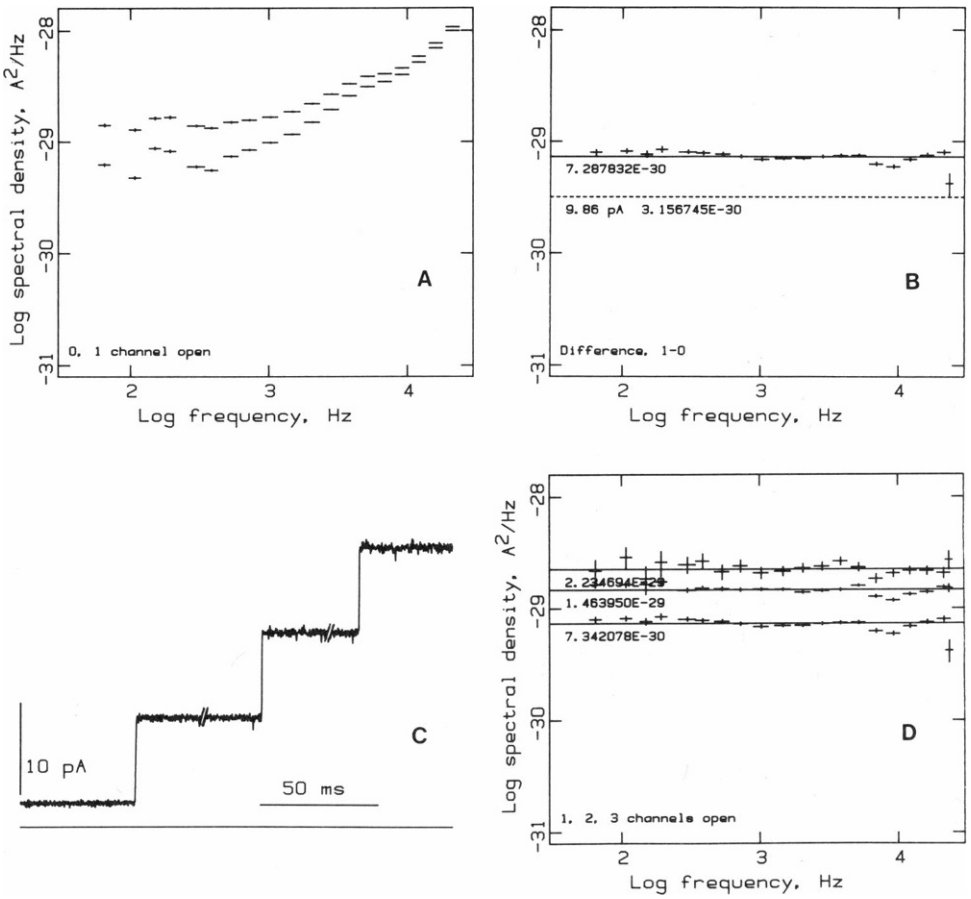

FIGURE 7 Difference spectra. (*A*) Average of a total of 1,256 1,024-point spectra obtained from record segments with no channels open (*lower points*), and of 1,296 spectra with one channel open to the main conductance state (*upper points*). The total duration of the record segments used to calculate the average spectra were 29 and 30 s, respectively. (*B*) Difference of the two spectra in *A*. The difference spectrum is flat and is considerably larger than the expected shot noise density (*dashed line*). (*C*). Illustration of the noise increase with channel number from zero to three. Data were Gaussian filtered at 2 kHz, and the vicinities of channel-opening transitions are shown juxtaposed. (*D*). Difference spectra obtained by subtracting the zero-channel background from average spectra at 1, 2, and 3 channels open. The fitted spectral densities were 7.3, 14.6, and 22.3 $\times$ 10^{-30} A^2/Hz, respectively. All data are from Ala^7 channels in 200 mM Cs, 200 mV; same run as in Fig. 3.

where r nearly doubled in 200 mM Cs. The increased noise in the Ala^7 is particularly intriguing, because although the current changed very little, the mechanism of ion transport in the channels is likely to be quite different at this lower ion concentration, and this might provide a clue to the origin of the excess noise.

Recordings were also made at a membrane potential of 100 mV. Again, all of the spectra were flat, but values of r were closer to unity, falling in the range of 1.15–1.3. The average spectral densities are plotted in Fig. 11 as a function of the mean channel current at 100 mV (*open symbols*) and 200 mV (*closed symbols*). The dashed line in each part of the figure gives the shot noise prediction, and increasing values of r would be represented by straight lines of increasing slope in this figure.

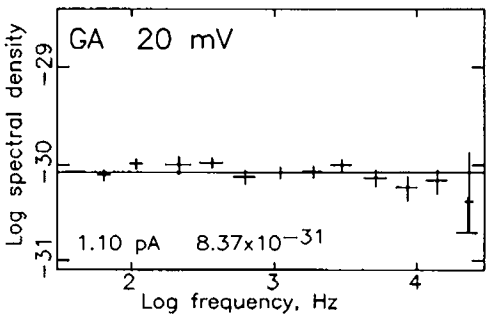

FIGURE 8 Near-equilibrium noise from a GA channel in 1 M Cs at 20 mV. The difference spectrum was calculated from a total of 30 s of open time (1,280 spectra were averaged) and 8 s of closed time (364 spectra). The line is drawn at the spectral density of 8.4 $\times$ 10^{-31} A^2/Hz, which is the average of the spectrum over the frequency range 500 Hz to 5 kHz. The mean current was 1.1 pA, corresponding to a conductance $\gamma \simeq 55$ pS; the Johnson (equilibrium) current noise from this conductance is expected to be $4kT\gamma = 8.8 \times 10^{-31}$ A^2/Hz.

DISCUSSION

The analysis presented here of open-channel noise in gramicidin and chemical analogues leads to two main conclusions. First, the spectra of this noise are flat, showing no obvious frequency dependence over the frequency range of 40 Hz to 20 kHz. Secondly, the value of the spectral density is higher than that expected for simple shot noise, with the discrepancy being factors between 1.1 and 2.4.

The observation of flat spectra stands in contrast to a previous study of noise in open gramicidin channels (Sauvé and Bamberg, 1978), where power spectra were obtained over the frequency range of 4-2000 Hz from membranes containing 10^2 to 10^6 channels. To avoid the on-off current fluctuations of gramicidin dimerization, these workers used the covalent dimer, malonyl-bis-desformylgramicidin (malonyl-GA), which forms channels of extremely long lifetime. Their spectra were fitted by the "$1/f$" function,

$$S(f) = \frac{\alpha I^2}{Nf},$$

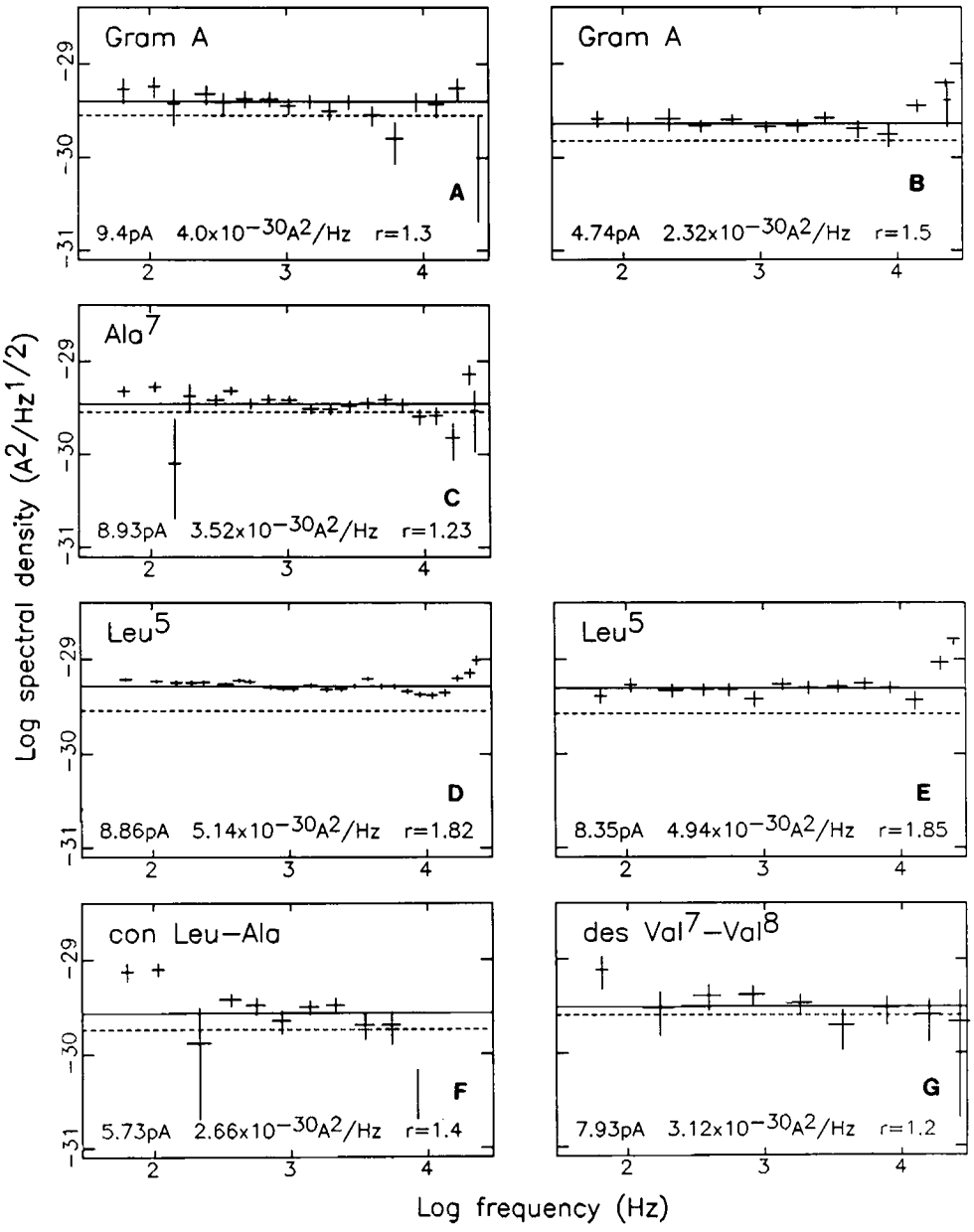

FIGURE 9 Difference spectra from GA and analogues in 1 M Cs, 200 mV. Spectra are shown for the main conductance levels except for panels *B* and *E*, which show spectra for low conductance states in GA and Leu[5]. Given with each spectrum is the mean current, the average spectral density (500 Hz to 5 kHz band), and the ratio *r* of the spectral density to the shot noise value. The data for the con Leu-Ala analogue were of poor quality, but the spectral density in the range 300 Hz to 3 kHz is flat and has an amplitude consistent with the other analogues.

where f is the frequency in Hertz, I is the total membrane current and N is the total number of channels. The constant α was evaluated to be $\simeq 10^{-2}$; taking $N = 1$ this predicts a spectral density of $1.2 \times 10^{-27} A^2/Hz$ at $f = 100$ Hz for a single channel, assuming the channel conductance $\gamma = 17$ pS for the malonyl-GA, and 200 mV membrane potential. This spectral density is 160 times the largest value observed in the present work (Fig. 10 *C*), even though the malonyl-GA channel's conductance is lower than that of the channels studied here. A likely explanation for the high spectral densities observed by Sauvé and Bamberg would be occasional transitions among different conductance levels in the malonyl-GA channels. Such transitions are observed in GA channels (Busath and Szabo, 1981) and are also present in malonyl-GA channels (Busath, D., personal communication). Stepwise conductance changes having suitable kinetics could give rise to multiple Lorentzian components in the power spectrum, giving a "$1/f$"-like spectrum (Sauvé and Szabo, 1982) of the magnitude that Sauvé and Bamberg observed. Our spectra would not have been contaminated in this way because the resolution of single channel events has allowed us to exclude stepwise current changes from the spectral analysis.

Brief Interruptions the Source of Excess Noise?

As will be shown in a succeeding paper (Sigworth, F., and J. Shenkel, manuscript in preparation), the predictions of the ion-transport schemes for Cs^+ in GA channels by Finkelstein and Andersen (1981) and by Eisenman and

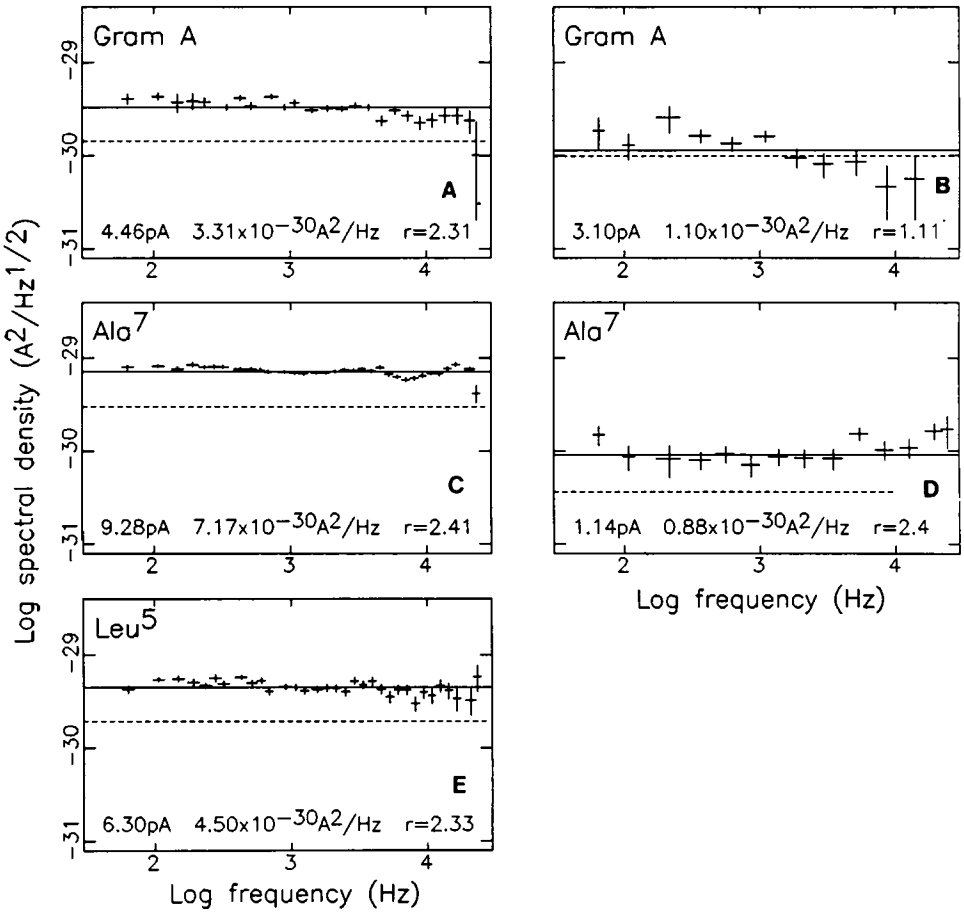

FIGURE 10 Difference spectra from GA, Ala[7] and Leu[5] channels in 200 mM Cs and 200 mV. Spectra from main levels are shown on the left; two spectra from sublevels are shown on the right. The Ala[7] analogue showed a much higher channel current than GA (9.3 pA vs. 4.5 pA) at this ion concentration.

Sandblom (1983) are for spectral densities very close to, or smaller than, the classical shot noise level. One explanation for the observation of spectral densities considerably above the shot noise level would be that the elementary transport event might involve the movement of more than one elementary charge. For example, if two monovalent ions moved simultaneously through the channel, Eq. 2 would predict twice the spectral density. This sort of process is unlikely for several reasons, not the least being that higher noise levels were observed at the lower permeant ion concentration that was used (Fig. 11). A more likely possibility is that the channel current undergoes brief interruptions (gaps) which, if they are brief enough, would contribute only a constant component to the spectral density in the frequency range that we have measured. Suppose that the current is interrupted completely during a gap, and that these gaps occur with an average frequency λ and have exponentially-distributed durations with mean τ. Assuming that, between the gaps, the channel satisfies the assumptions of the Schottky theory, the power spectrum of the current fluctuations is given by:

$$S(f) = 2iq + 4\lambda\tau^2 i^2 \frac{1}{1 + (f\tau/2\pi)^2}, \qquad (3)$$

where the mean current i is related to the unblocked channel current i_0 by

$$i = (1 - \lambda\tau)i_0.$$

(Here terms of second order in $\lambda\tau$ have been neglected.) The first term in Eq. 3 is the shot noise, and the second term is a Lorentzian function arising from the exponentially-distributed gap durations. If τ is brief compared with the time resolution of the recording, the frequency dependence can be neglected altogether, and taking the limit as $f \rightarrow 0$

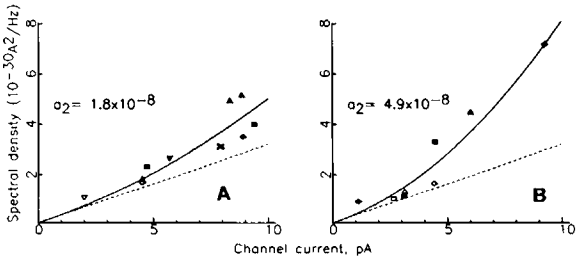

FIGURE 11 Current dependence of average spectral density. Spectral density is plotted as a function of channel current for recordings at 200 mV (*solid symbols*) and 100 mV (*open symbols*). (*A*) Data obtained in 1 M Cs; (*B*) data from 200 mM Cs. The various symbols represent analogues as follows: GA, □; Leu[5], △; Ala[7], ◇; des Val[7]-Val[8], ×; con Leu-Ala, ▽. The dashed line shows the expected shot noise; the solid curves are drawn according to Eq. 4 with the values given for the quadratic term $a_2 = \lambda\tau^2$.

the spectral density is seen to depend on i according to

$$S = 2iq + 4\lambda\tau^2 i^2. \quad (4)$$

The spectral density data in Fig. 11 are plotted for comparison with this theory. In each part of the figure the dashed line shows the first (shot noise) term of Eq. 4, and the solid curve the sum of both terms for particular values of the product $a_2 = \lambda\tau^2$. The product was taken to be 1.8×10^{-8} s in part *A*, and 4.9×10^{-8} s in part *B*. The higher value for the 200-mM data in part *B* would be interpreted to mean that the gap duration or frequency is higher at the lower ion concentration.

As was shown in Fig. 5, currents in GA and its analogues do in fact have brief gaps that can be resolved in our recordings, but the masking procedure that we used removed most of them from the data before power spectra were computed. The population of brief gaps in Fig. 6 *A* had $\tau = 27$ μs and $\lambda = 8.2$ s^{-1}, which would result in a substantial contribution of 1.2×10^{-30}A^2/Hz to the spectrum. However, the masking procedure, by a conservative estimate, eliminated all gaps shorter than 15 μs; the contribution S_g of the remaining gaps, with random durations t_g, to the spectrum can be calculated as:

$$S_g = 2\lambda \langle t_g^2 \rangle i^2,$$

where truncated-exponential probability distributions were assumed for the gap dwell times in evaluating the expectation value $\langle t_g^2 \rangle$. The result is $S_g = 4.5 \times 10^{-32}$ A^2/Hz, two orders of magnitude smaller than the corresponding spectral density of GA channels measured in 1 M Cs and 200 mV. Similarly, the gap parameters from Fig. 6 *B* result in $S_g = 1.5 \times 10^{-31}$A^2/Hz, also much smaller than the measured Ala^7 spectral density.

The values of a_2 obtained as in Fig. 11, along with the observed distribution of gap durations (Fig. 6), place constraints on the kinetics of gaps that could give rise to the observed excess noise. One limit is that the gaps must be shorter than 3 μs in mean duration; otherwise they would contribute large numbers of events in the lowest bins of the histograms of Fig. 6. Taking the case of Ala^7 in 200 mM Cs (Fig. 6 *B*), the constraint of $\lambda\tau^2 = 5 \times 10^{-8}$ s requires that $\lambda = 5{,}000$ s^{-1} if $\tau = 3$ μs. This high rate of occurrence would yield five events per second of duration >20 μs, doubling the size of the second bin in the histogram; the first bin would show an even larger excess and the deviation from an exponential distribution would be obvious. On the other hand a lower limit on the gap duration of ~50 ns is set by the requirement that $\tau < \lambda^{-1}$, i.e., that there must be time for the channel to conduct in between gaps. In this limit the channel would behave as if the permeating species had a valence >1, since it would spend most of its time closed, and during each brief conducting interval a group of several ions would be transported in rapid succession.

The excess noise could arise from smaller or more gradual changes in conductance than the complete interruptions assumed above, but in this case the kinetics would have to be at least as rapid. For example, half-closures of the channel would need four times the value of λ as complete closures, to result in the same amount of noise for a given value of τ. As a working hypothesis we favor the idea that essentially complete closures are the most likely result of whatever structural fluctuations are causing the excess noise. In support of this is the observation that quite small changes in barrier energies can cause large reductions in conductance (Urry 1985*b*).

The various possibilities for the value of τ could be distinguished if spectral data were available to higher frequencies, since the corner frequency of the spectrum would reflect τ; unfortunately, even the longest value of $\tau = 3$ μs corresponds to a corner frequency of 50 kHz, well above the bandwidth of our measurements. However, there are ways to obtain indirect estimates for τ, and these will be considered in a subsequent paper.

We thank Dr. E. Neher for his advice and hospitality, as most of the experimental work was done in his laboratory.

This work was supported by an award from the Alexander von Humboldt Stiftung to D. W. Urry, and by National Institutes of Health grants GM26898 and NS21501.

Received for publication 10 February 1987 and in final form 13 August 1987.

REFERENCES

Andersen, O. S. 1983. Ion movement through gramicidin A channels: single channel measurements at very high potentials. *Biophys. J.* 41:119–133.

Andersen, O. S. 1984. Gramicidin channels. *Annu. Rev. Physiol.* 46:531–548.

Bezanilla, F. 1985. A high capacity data recording device based on a digital audio processor and a video cassette recorder. *Biophys. J.* 47:437–441.

Busath, D., and G. Szabo. 1981. Gramicidin forms multi-state rectifying channels. *Nature (Lond.).* 294:371–373.

Colquhoun, D., and F. J. Sigworth. 1983. Fitting and statistical analysis of single-channel records. *In* Single Channel Recording. B. Sakmann and E. Neher, editors. 191–263. Plenum Publishing Corp., New York.

Eisenman, G., and J. Sandblom. 1983. Energy barriers in ionic channels: data for gramicidin A interpreted using a single-file (3B4S″) model having 3 barriers separating 4 sites. *In* Physical Chemistry of Transmembrane Ion Motions. G. Sprach, Editor. Elsevier North-Holland, Inc., New York. 329–348.

Finkelstein, A., and O. S. Andersen. 1981. The gramicidin A channel: a review of its permeability characteristics with special reference to the single-file aspect of transport. *J. Membr. Biol.* 59:155–171.

Hamill, O. P., A. Marty, E. Neher, B. Sackmann, and F. G. Sigworth. 1981. Improved patch-clamp techniques for high resolution current recording from cells and cell-free membrane patches. *Pfluegers Arch. Eur. J. Physiol.* 391:85–100.

Hladky, S. B., and D. A. Haydon. 1972. Ion transfer across lipid membranes in the presence of gramicidin A. *Biochim. Biophys. Acta.* 274:294–312.

Hladky, S. B., and D. A. Haydon. 1984. Ion movements in gramicidin channels. *Curr. Top. Membr. Trans.* 21:327–372.

Läuger, P. 1975. Shot noise in ion channels. *Biochim. Biophys. Acta.* 413:1–10.

Neher, E., B. Sakmann, and J. H. Steinbach. 1978. The extracellular patch clamp: a method for resolving currents through individual open

channels in biological membranes. *Pfluegers Arch. Eur. J. Physiol.* 375:219–228.

Prasad, K. U., T. L. Trapane, D. Busath, G. Szabo, and D. W. Urry. 1982. Synthesis and characterization of 1-^{13}C-D·Leu^{12,14} gramicidin A. *Int. J. Pept. Protein Res.* 19:162–171.

Prasad, K. U., S. Alonso-Romanowski, C. M. Venkatachalam, T. L. Trapane, and D. W. Urry. (1986). Synthesis, characterization and BLM studies of L·Ala^7-Gramicidin A. *Biochemistry.* 25:456–463.

Ring, A. 1986. Brief closures of gramicidin A channels in lipid bilayer membranes. *Biochim. Biophys. Acta.* 856:646–653.

Schottky, W. 1918. *Ann. Phys. (Leipzig).* 57:541–567.

Sigworth, F. J. 1985. Open channel noise. I. Noise in acetylcholine receptor currents suggests conformational fluctuations. *Biophys. J.* 47:709–720.

Sigworth, F. J. 1986. Open channel noise. II. A test for coupling between current fluctuations and conformational transitions in the acetylcholine receptor. *Biophys. J.* 49:1041–1046.

Sigworth, F. J., and S. M. Sine. 1987. Data transformations for improved display and fitting of single-channel kinetics. *Biophys. J.*52:000–000.

Stevens, C. F. 1972. Inferences about membrane properties from electrical noise measurements. *Biophys. J.* 22:1028–1047.

Urry, D. W. 1971. The gramicidin A transmembrane channel: a proposed $\pi_{(L,D)}$ helix. *Proc. Natl. Acad. Sci. USA.* 68:672–676.

Urry, D. W., M. C. Goodall, J. D. Glickson, and D. F. Mayers. 1971. The gramicidin transmembrane channel: characteristics of head-to-head dimerized $\pi_{(L,D)}$ helices. *Proc. Natl. Acad. Sci. USA.* 68:1907–1911.

Urry, D. W., S. Alonso-Romanowski, C. M. Venkatachalam, T. L. Trapane, and K. U. Prasad. 1984*a*. The source of the dispersity of gramicidin A single-channel conductances: the L-Leu^5-gramicidin A analog. *Biophys. J.* 46:259–265.

Urry, D. W., S. Alonso-Romanowski, C. M. Venkatachalam, R. D. Harris, and K. U. Prasad. 1984*b*. Dispersity of des-L-Val^7-D-Val^8-gramicidin A single channel conductances argues for different side chain orientations as basis. *Biochem. Biophys. Res. Commun.* 118:885–893.

Urry, D. W. 1985*a*. Chemical basis of ion transport specificity in biological membranes. *Topics Curr. Chem.* 128:175–218.

Urry, D. W. 1985*b*. On the molecular structure of the gramicidin transmembrane channel. *In* The Enzymes of Biological Membranes. A. N. Martonosi, editor. 229–257. Plenum Publishing Corp., New York.

Urry, D. W., T. L. Trapane, C. M. Venkatachalam, and R. B. McMichens. 1988. Ion interactions at membranous polypeptide sites using NMR: determining rate and binding constants and site locations. *Methods Enzymol.*

Venkatachalam, C. M., S. Alonso-Romanowski, K. U. Prasad, and D. W. Urry. 1984. The Leu^5 gramicidin A analog: molecular mechanics calculations and analysis of single channel steps related to multiplicity of conducting states. *Int. J. Quantum Chem. Symp.* 11:315–326.